

Subjective Camera: Bridging Human Cognition and Visual Reconstruction through Sequence-Aware Sketch-Guided Diffusion

Haoyang Chen^{1,2*} Dongfang Sun^{1,2*} Caoyuan Ma^{1,2*} Shiqin Wang³ Kewei Zhang^{1,2}
Zheng Wang^{1,2†} Zhixiang Wang^{4†}

¹National Engineering Research Center for Multimedia Software, Institute of Artificial Intelligence, School of Computer Science, Wuhan University ²Hubei Key Laboratory of Multimedia and Network Communication Engineering
³Wuhan University of Science and Technology ⁴National Institute of Informatics, Tokyo

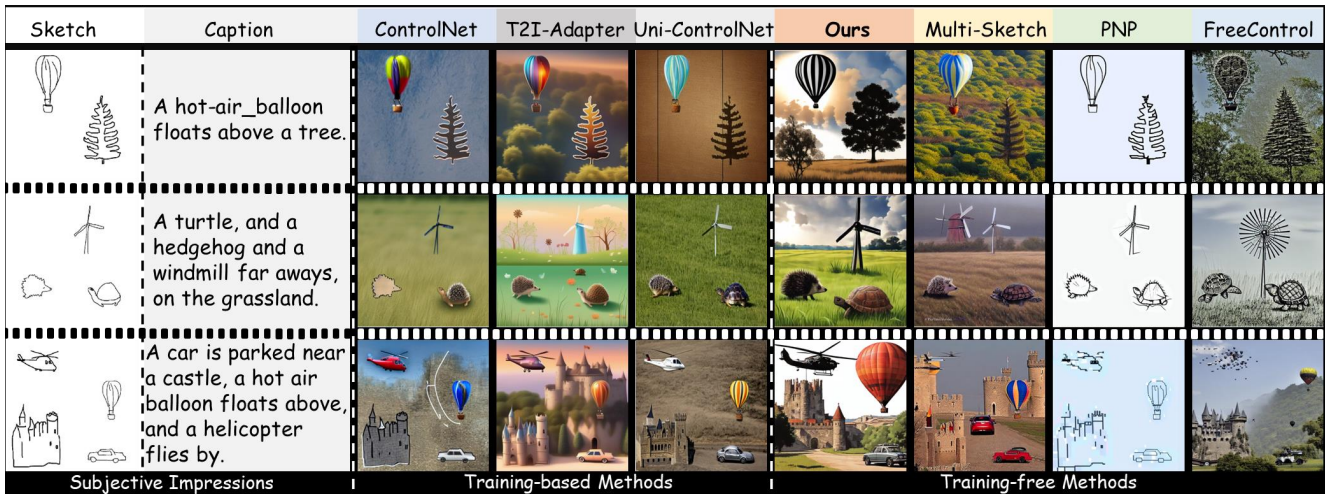


Figure 1. **Subjective Camera: Translating Mental Impressions into Photorealistic Images.** Our approach overcomes limitations of existing training-based [10, 20, 24] and training-free methods [1, 9, 15] by leveraging synergistic use of verbal descriptions and rough sketches to reconstruct real-world scenes. In contrast to existing approaches that exhibit limitations such as susceptibility to sketch biases, sensitivity to input quality, presence of conspicuous artifacts, and failure in geometric consistency, Subjective Camera demonstrates a novel capability to transform subjective perceptual representations into photorealistic imagery while eliminating the necessity for model fine-tuning or specialized artistic skills.

Abstract

We propose *Subjective Camera*, a human-as-imaging-device paradigm that reconstructs real-world scenes from mental impressions through synergistic use of verbal descriptions and progressive rough sketches. This approach overcomes dual limitations of language ambiguity and sketch abstraction by treating the user’s drawing sequence as priors, effectively translating subjective perceptual expectations into photorealistic images.

Existing approaches face three fundamental barriers: (1) user-specific subjective input biases, (2) huge modal-

ity gap between planar sketch and 3D priors in diffusion, and (3) sketch quality-sensitive performance degradation. Current solutions either demand resource-intensive model adaptation or impose impractical requirements on sketch precision.

Our framework addresses these challenges through concept-sequential generation. (1) We establish robust appearance priors through text-reward optimization, and then implement sequence-aware disentangled generation that processes concepts in sketching order; these steps accommodate user-specific subjective expectation in a training-free way. (2) We employ latent optimization that effectively bridges the modality gap between planar sketches and 3D priors in diffusion. (3) Our hierarchical reward-

*These authors contributed equally to this work.

†Corresponding authors.

guided framework enables the use of rough sketches without demanding artistic expertise. Comprehensive evaluation across diverse datasets demonstrates that our approach achieves state-of-the-art performance in maintaining both semantic and spatial coherence.

1. Introduction

Humans use cameras to preserve memorable moments. However, a physical camera cannot capture every moment. These moments live on in our memories. It would be fun and extremely rewarding to recreate these scenes from our minds faithfully! Therefore, this paper is the first to propose the concept of a **Subjective Camera**, where humans function as imaging devices guided by their subjective consciousness, aiming to accurately reconstruct real-world scenes based on their personal impressions and memories.

The most expeditious way to share a mental scene with others is through verbal description, yet it alone is hard to express users' preferences and intentions in content creation, especially object layout and details. Freehand sketches, due to their simplicity, low cost, and ability to directly or indirectly reflect objective realities, serve as the preferred form of external signal [8, 19]. However, the effectiveness of freehand sketches is often limited by the user's drawing skills, which can lead to inconsistencies in geometric representation. This limitation, combined with the ambiguity of verbal descriptions, presents a dual challenge in accurately capturing user subjective intentions.

Existing methods can be broadly categorized into two types. The first type [10, 17, 20, 23, 24] minimizes reconstruction errors by brute-force learning. However, this approach is constrained by the need for large-scale freehand sketch-image pairs, leading to high training costs, an inability to handle the inherent subjective biases in hand-drawn sketches from different users, and limited generalization to abstract sketches due to specific training data distribution. The others explore training-free alternatives to circumvent these challenges. Cheng *et al.* [1] employed a pre-trained ControlNet [20] to guide the generation of foreground objects and background regions using foreground masks. Similarly, Zhang *et al.* [22] incorporated the spatial information of sketches into the attention layers of the pre-trained Latent Diffusion Model as the condition for image generation. However, these methods heavily depend on the quality of the sketches and tend to fit to the sketches, making them vulnerable to abstract input (rough sketches). Moreover, both categories employ simultaneous denoising of multiple foreground objects, which leads to layout deviations between generated results and user intent in sketch, as illustrated in Figure 1. In summary, all existing methods encounter challenges stemming from three main issues: (1) the subjective biases present in sketches from differ-

ent users, (2) the need for user sketches to be of sufficient quality, and (3) the lack of effective strategies to bridge the modality gap between the concepts in planar sketches and those in real images which involve inherent 3D real-world prior.

Our key insight stems from the observation that the user's free-hand sketching process inherently encapsulates their subjective intention, that is, **the order of sketch creation matters**. We observe that users tend to employ text to describe overall scene information, while sketches reflect the user's expectations regarding concept layout and shape, with initially drawn concepts receiving greater attention. For example, users might first sketch a cat before adding trees and benches, indicating the cat's priority in the composition. To generate realistic images that align with any user's subjective expectations, we propose a multi-stage training-free diffusion framework that leverages the sequence of user-drawn concepts. This framework progressively guides the evolution from abstract planar sketches to photorealistic images through concept-sequence-aware training-free guidance, ensuring alignment with both real-world priors and user intent.

We decouple the Subjective Camera into three key aspects: the appearance, shape, and layout of concepts. The input consists of two components: 1) a user-defined textual description capturing their subjective perception of the scene, and 2) a progressively drawn (probably rough) sketch that encodes the user's expectation about the shapes and spatial arrangements of concepts. Specifically, since the Subjective Camera lacks precise input for concept appearance, we first leverage the textual description to derive an appearance prior for the following steps through a text-to-image (T2I) model (Sec. 3.2). This process integrates subjective descriptions with the rich real-world image distribution embedded in the pre-trained model. Subsequently, we utilize Sequence-Aware Disentangled Generation (Sec. 3.3). The spatial latent representations (layout and shape) from the last concept dynamically influence the following constituents, thereby preserving subjective expectation. To bridge the modality gap, we employ Latent Optimization (Sec. 3.4) to align planar sketch concepts with shape-approximated real-world objects. This noise injection preserves macroscopic spatial intention while introducing real-world priors to mitigate cross-modal discrepancies. Our hierarchical reward-guided framework focuses on capturing user expectations from the abstract input rather than sketch line details, making our model accessible with rough sketch and text description. Comprehensive evaluation across diverse datasets demonstrates that our approach achieves state-of-the-art performance in maintaining both semantic and spatial coherence.

In conclusion, our contributions can be summarized as follows:

- **Novel Paradigm of Subjective Camera:** We pioneer the concept of a *Subjective Camera* that transforms human cognition into a generative computational imaging process. This work bridges episodic memory and visual reconstruction through temporally-encoded sketch sequences and textual semantics, establishing new foundations for cognitive-driven image generation.
- **Multi-stage train-free Diffusion Framework:** Our coarse to fine framework with multi-stage rewards, enables the model to focus on the user’s true intent rather than the line details in the sketch.
- **Zero-Shot Multi-Modal Alignment:** We hierarchically fuses semantic anchors from text prompts with spatial-temporal sketch patterns. This innovation overcomes dual constraints of limited sketching skills and verbal expression capabilities, achieving robust alignment without dataset-specific training.

2. Related Work

2.1. Sketch-to-Image Generation

The task aims to generate corresponding real-world images from free-hand sketches based on textual prompts. With the emergence of pre-trained T2I diffusion models, such as Stable Diffusion [12], their powerful semantic understanding and content generation capabilities have significantly advanced the development of this task. Existing researchers fine-tuned frozen pretrained T2I diffusion models via training extra modules [17, 20] (or adapters [10, 24]), or directly trained the diffusion model via minimizing the reconstruction errors [23]. In detail, Zhang *et al.* [20] fine-tuned the pre-trained T2I diffusion model by adding and training a trainable copy of its encoding layers to learn task-specific conditions. Mou *et al.* [10] proposed T2I-Adapter which was trained to align internal knowledge in the T2I model with condition features from input sketches. Similarly, Zhao *et al.* [24] designed Uni-ControlNet that fine-tuned the local control adapter and global control adapter on a frozen pre-trained T2I diffusion model, respectively. Zhang *et al.* [23] trained the diffusion model by inputting masks of all foreground objects, enabling it to focus on foreground regions generation via reconstruction loss. Despite their superior performance, these training-based methods bring high training costs and poor scalability. Training-free methods [1, 9, 22] have emerged to solve these issues. Multi-Sketch [1] utilized a pre-trained ControlNet to complete the sampling process, where foreground objects and background regions are separately denoised and then fused. Zhang *et al.* [22] fed sketch label and positional information into the attention layers of a latent diffusion model to offer spatial guidance for image generation. FreeControl [9] introduced structure and appearance guidance to progressively update the noise component during the sam-

pling phase. However, these training-free methods jointly denoise multiple concepts in sketches, causing interference in their noise characteristics and preventing each element from achieving optimal learning outcomes.

All above existing methods struggle to eliminate subjective biases across users and are highly susceptible to highly abstract sketches, leading to appearance deviations and semantic inconsistencies in generated images.

2.2. Reward Optimization

Recently, fine-tuning T2I models using reward objectives has garnered significant attention from researchers [2, 3, 6, 7, 14, 18] due to its ability to optimize models based on specific preferences. Early works [6, 18] directly fine-tuned diffusion models using differentiable rewards. Later, to circumvent the challenges of fine-tuning model parameters, some works [2, 3, 7, 14] directly optimize the initial latent noise. CoCoNO [14] utilized the designed attention complete loss and attention contrast loss to update the parameters of the initial latent noise. InitNO [3] first identified valid regions in the initial latent space and employed the designed distribution alignment loss to guide the initial noise towards these regions. ReNO [2] iteratively updated the initial latent noise by maximizing the reward scores of images generated by the frozen T2I model. However, these methods, designed for text-to-image tasks, fail to effectively constrain the positional information of concepts in sketches, making them unsuitable for image-to-image (*e.g.*, sketch-to-image) generation tasks.

3. Subjective Camera

3.1. Method Overview

We present a Subjective Camera that faithfully “reconstructs” scenes from people’s minds without requiring professional writing or drawing skills from users. Specifically, for a given text prompt p and sketch concepts list S , the Subjective Camera empowers a pre-trained T2I diffusion model \mathcal{G} to generate realistic images aligned with p that maintain semantic and spatial structures conforming to users’ subjective expectations. However, generating images based solely on simple text descriptions and abstract sketches that meet users’ subjective expectations presents significant challenges. These challenges involve not only bridging the substantial modality gap between text-sketch inputs and real-world images but also satisfying users’ subjective expectations throughout this process.

Our key insight lies in recognizing that the user’s textual descriptions and the sequential order of sketch inputs inherently encode their expectations and focus regarding the target scene. Therefore, we design a coarse-to-fine three-stage approach to accomplish this challenging task. First, lacking explicit appearance guidance (color, texture), we lever-

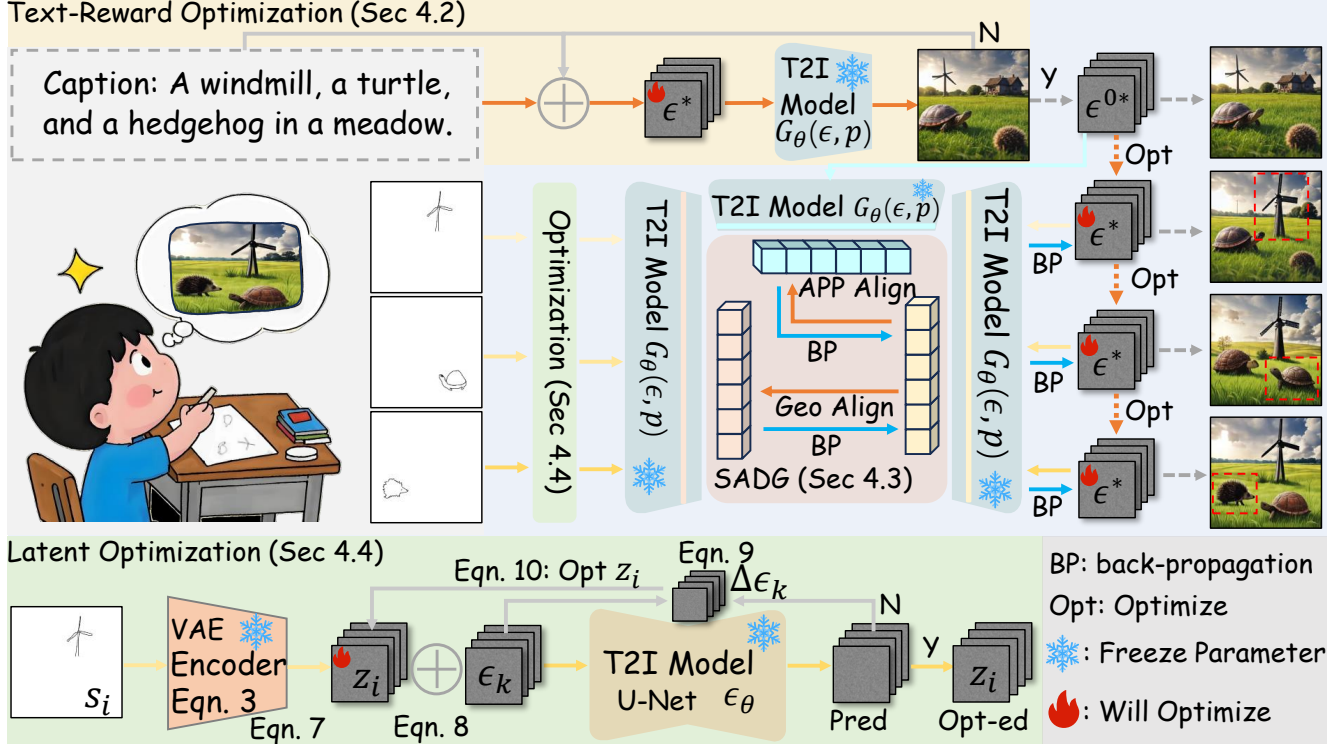


Figure 2. **Subjective Camera.** Our framework formalizes human-as-imager cognition through sequential alignment: (1) User-provided sketches and verbal descriptions undergo text-reward optimization (Sec. 3.2) to extract appearance priors ϵ^{0*} via iterative noise refinement; (2) Generation progresses under dual constraints - spatial layout conforming to sketch topology while appearance details adhere to ϵ^{0*} , with temporal consistency maintained through ordered latent propagation that respects the drawing chronology, ensuring coherent integration of emerging and established scene elements (Sec. 3.3); (3) The sketch sequence drives latent space alignment through diffusion knowledge injection (Sec. 3.4), bridging the modality gap between creative abstraction and physical reality; .

age textual descriptions through pre-trained T2I models to generate images that simultaneously conform to real-world priors and users’ subjective preferences. This text reward optimization process provides appearance information for subsequent sketch-guided processes, as we observe that text contains more information about concept appearance while sketches primarily provide shape, structure, and spatial distribution guidance. Subsequently, we generate content according to the order in which users draw concepts—what we term concept-sequence awareness—using training-free guidance enhanced by our spatial attention-guided reward strategy to control each concept’s generation process. This approach simultaneously coordinates the model’s understanding of both new and existing elements, naturally aligning with the sequential input of concepts. For each concept’s generation, we employ single-step noise guidance for modality alignment, transforming planar abstractions from sketches into noise corresponding to 3D entities with similar spatial information. This ensures that the final generated results satisfy user expectations while incorporating physical world priors.

We formalize the Subjective Camera as a parametric

mapping \mathcal{F} that synthesizes photorealistic images from textual prompts p and freehand sketch sequences $S = \{s_i\}_{i=1}^N$:

$$I = \mathcal{F}(p, S; \epsilon_g, \mathcal{A}) \quad (1)$$

where \mathcal{A} represents the appearance prior derived from p , and ϵ_g denotes the geometric prior inferred from the temporal order of sketch sequence S . This differentiable formulation establishes a principled connection between human-centric abstraction and visual realism while maintaining intentional fidelity.

3.2. Text-Reward Optimization

The initial stage of our approach involves extracting appearance information from textual descriptions, which serves as a crucial foundation for subsequent sketch-guided processes. We observe that while sketches primarily provide shape, structure, and spatial distribution guidance, they lack explicit appearance information such as color, texture, and lighting details. Text prompts, on the other hand, often contain rich semantic cues about visual attributes that inform the subjective expectations of users.

To leverage this textual information effectively, we formulate a text-reward optimization procedure that extracts appearance priors through iterative refinement of latent noise. Given a text prompt p , we optimize an initial noise vector ϵ to maximize a text-image alignment score:

$$\epsilon^* = \arg \max_{\epsilon} \mathcal{C}_F(\mathcal{G}_\theta(\epsilon, p)), \quad (2)$$

where \mathcal{G}_θ denotes our pre-trained text-to-image diffusion model, and \mathcal{C}_F represents a CLIP-based differentiable evaluation function that measures semantic alignment between the generated image and the text prompt p .

The optimization process iteratively refines ϵ through gradient ascent:

$$\epsilon_{t+1} = \epsilon_t + \eta \nabla_{\epsilon} \mathcal{C}_F(\mathcal{G}_\theta(\epsilon_t, p)), \quad (3)$$

where η is the learning rate.

The optimized noise vector ϵ^* encodes rich appearance information derived from the text prompt, serving as the appearance prior \mathcal{A} in our framework. \mathcal{A} guides subsequent stages by providing a reference for visual attributes such as color, texture, and lighting, which are critical for generating photorealistic images that align with users' mental models. By extracting these appearance cues from text through optimization, we establish an appearance foundation that complements the structural information provided by sketches, facilitating a more comprehensive reconstruction of the scene envisioned by the user.

3.3. Sequence-Aware Disentangled Generation

After establishing \mathcal{A} , we address the challenge of incorporating multiple sketch concepts in a sequential, orderly manner that respects the user's drawing process. The order in which users sketch concepts inherently reflects their focus and priorities regarding the scene's composition. Our sequence-aware disentangled generation approach leverages this temporal information to progressively build the scene while maintaining coherence between newly introduced and previously established elements.

Spatial Attention-Guided Control. The key to our sequence-aware generation lies in leveraging the spatial attention mechanisms within the diffusion model's UNet architecture. For each sketch concept s_i , we extract cross-attention maps that highlight regions in the latent space corresponding to specific semantic concepts:

$$\mathcal{M}_i = \left\{ y \mid \left[\text{softmax} \left(\frac{QK^T}{\sqrt{d}} \right) \right]_{i,y} > \tau \right\}, \quad (4)$$

where Q and K are query and key matrices derived from image features and text embeddings respectively, d is the dimensionality of the key vectors, and τ is a threshold parameter. These attention maps \mathcal{M}_i serve as spatial indicators to guide the concept layout.

Sequential Concept Integration. To maintain coherence across the progressive addition of concepts, we implement a sequential integration process that updates the latent noise representation while preserving previously incorporated elements. For each sketch s_i in the sequence, we compute:

$$\epsilon_i^* = \epsilon_{i-1}^* + \Delta \epsilon_i, \quad (5)$$

where ϵ_{i-1}^* is the optimized noise from the previous step, and $\Delta \epsilon_i$ represents the incremental update required to incorporate the current sketch concept latent feature z_i derived from s_i (elaborated in Sec. 3.4). This update is guided by our energy function:

$$\mathcal{E}_i = \alpha_i \mathcal{L}_{\text{new}}(z_i, \epsilon_i^*) + \beta_i \sum_{j=1}^{i-1} \gamma^{i-j} \mathcal{L}_{\text{preserve}}(z_j, \epsilon_i^*), \quad (6)$$

where \mathcal{L}_{new} ensures proper integration of the current z_i , $\mathcal{L}_{\text{preserve}}$ maintains the integrity of previously added z_j , α_i and β_i are balancing coefficients, and γ^{i-j} is a decay factor that weights the importance of preserving earlier concepts based on their temporal distance from the current step.

By processing sketches in sequence and maintaining awareness of their temporal order, our approach naturally aligns with the human creative process, enabling users to incrementally construct imagined scenes while ensuring each addition respects and complements previous elements. This sequence-aware generation strategy enables precise control over complex multi-concept scenes while preserving the user's subjective intent encoded in the drawing order.

3.4. Latent Optimization

In this section, we propose a novel approach to bridge the modality gap between human creativity and physical world by injecting the pre-trained knowledge of diffusion models, without requiring additional training. Formally, given a list of input sketches $\{s_i\}_{i=1}^N$, each sketch s_i is encoded into a latent representation $z_i \in \mathbb{R}^{h \times w \times d}$ using the variational autoencoder (VAE) encoder E_ϕ of the diffusion model:

$$z_i = E_\phi(s_i) + \xi_i; \quad \xi_i \sim \mathcal{N}(0, \Sigma_\phi), \quad (7)$$

where $\Sigma_\phi = \text{diag}(\sigma_1^2, \dots, \sigma_d^2)$ quantifies the VAE's reconstruction uncertainty, ensuring robustness to noisy or incomplete sketches.

Noise-Aware Optimization. To address the significant domain gap between abstract planer sketches and realistic images, we introduce a noise-aware optimization procedure that iteratively refines the latent representation z_i by aligning it with the rich prior knowledge embedded in the diffusion model. At each optimization step k , we perturb the latent sketch representation with Gaussian noise $\epsilon_k \sim \mathcal{N}(0, \mathbf{I})$ to obtain a noisy latent representation $z_t^{(k)}$:

$$z_t^{(k)} = \alpha_{t_k} z_i^{(k)} + \sigma_{t_k} \epsilon_k, \quad (8)$$



Figure 3. **Qualitative comparison** of existing sketch-to-image training-based & training-free methods, and our method on FMC dataset. Existing training-based methods, such as ControlNet [20], T2I-Adapter [10], and Uni-ControlNet [24], fail to strictly adhere to textual descriptions. Training-free methods struggle to eliminate subjective biases, leading to inconsistencies between content and background in Multi-Sketch [1], difficulties in accurately reconstructing backgrounds according to textual descriptions in PNP [4], and blurred content edges in FreeControl [9]. In comparison, our approach more faithfully represents real-world physical scenes.

where α_{t_k} and σ_{t_k} are time-dependent scaling factors following the noise schedule of the diffusion process. The noisy latent $z_t^{(k)}$ is then fed into the pre-trained U-Net ϵ_θ , which predicts the noise component $\hat{\epsilon}_\theta(z_t^{(k)}, t_k)$. The noise prediction error $\Delta\epsilon_k$ is computed as:

$$\Delta\epsilon_k = \hat{\epsilon}_\theta(z_t^{(k)}, t_k) - \epsilon_k. \quad (9)$$

This noise gap serves as a gradient signal to iteratively refine the latent sketch features. Specifically, we update the latent representation $z_i^{(k)}$ via a geometrically tempered gradient descent:

$$z_i^{(k+1)} = z_i^{(k)} - \eta_k \left(\Delta\epsilon_k + \lambda(z_i^{(k)} - z_i^{(0)}) \right), \quad (10)$$

where λ is a regularization term that anchors the optimization to the initial latent $z_i^{(0)}$, preventing semantic drift. and η_k is an adaptive learning rate that decays exponentially with the gradient norm as follows:

$$\eta_{k+1} = \eta_k \cdot \exp(-\mu \|\Delta\epsilon_k\|_2), \quad (11)$$

where μ is an adjustable factor controlling intensity.

From Equation 8 to Equation 10, this process is formulated as an iterative optimization. Through this optimization, z_i is progressively aligned with the rich prior knowledge embedded in the diffusion model. This alignment effectively infuses the sketch with realistic details, textures, and structural coherence, thereby establishing a robust mapping from human hand-drawn sketches to physically grounded visual representations.

The latent optimization process serves as the bridge between the abstract sketch representations and realistic image

features. By leveraging the diffusion model’s learned priors, we transform simplified sketch concepts into nuanced, detailed visual elements that maintain their spatial and semantic integrity while gaining photorealistic appearance qualities. This optimization is critical for ensuring that the final generated image not only adheres to the user’s subjective intent as expressed through their sketches but also exhibits the physical plausibility and visual richness expected in real-world photographs.

4. Experiments and Results

4.1. Experiment Setup

4.1.1. Datasets

To rigorously evaluate the performance of our Subjective Camera, we have undertaken extensive efforts to develop two specialized datasets: the **Composed Multi-Concept (CMC)** dataset and the **Freehand Multi-Concept (FMC)** dataset. Both datasets are designed to comprehensively assess the capabilities of our framework in handling multi-concept scene understanding and generation. These datasets will be made publicly available to support further research and benchmarking in the community.

CMC Dataset: The CMC dataset comprises 142 scene sketches, each containing 2–4 distinct concepts sampled from the 150 semantic classes in the Sketchy dataset [13]. Each accompanied by manually annotated textual prompts with the help of visual Large language models. Unlike traditional datasets, the CMC dataset does not provide real-world ground-truth images as reference, making it suitable for subjective evaluation tasks such as human perception studies or qualitative analysis.

Method	CMC			FMC			
	FID ↓	CLIP ↑	HPS ↑	FID ↓	CLIP ↑	HPS ↑	LPIPS ↑
Training-based Methods							
ControlNet [20]	15.2800	61.7128	0.7940	14.4487	66.8048	0.8024	0.7671
T2I-Adapter [10]	18.1251	61.6142	0.7445	15.3720	61.6142	0.7445	0.5875
Uni-ControlNet [24]	19.5964	62.5783	0.7613	18.5307	62.5783	0.7613	0.8083
Training-free Methods							
Multi-Sketch [1]	13.0463	64.1083	0.7402	11.5891	72.0212	0.7748	0.7327
PNP [15]	17.0074	63.2696	0.8397	16.2610	71.2361	0.8516	0.5700
FreeControl [9]	14.5215	64.7380	0.7572	11.1713	66.6719	0.7585	0.8198
Subjective Camera (Ours)	11.5591	66.6376	0.8502	10.1849	74.2532	0.8620	0.8277

Table 1. Quantitative results on our CMC and FMC datasets. Our Subjective Camera consistently surpasses all training-free methods [1, 9, 15] in distribution matching, image-text alignment, subjective quality and appearance details by as measured by FID, CLIP, HPS and LPIPS. Subjective Camera achieves superior image-text alignment compared to training-based methods [10, 20, 24] (‘↓’ indicates lower values are better, while ‘↑’ signifies higher values are preferred).

FMC Dataset: The FMC dataset is constructed from free-hand sketches drawn by volunteers, based on real-world images sourced from publicly available outdoor scene datasets. It comprises 42 hand-drawn sketches, each containing 2-3 distinct concepts. Additionally, each sketch is paired with a corresponding real-world image as ground-truth reference for validation and evaluation purposes.

4.1.2. Evaluation Metrics

To conduct a comprehensive quantitative evaluation of the quality of generated images, four widely-used evaluation metrics were employed, including Fréchet Inception Distance (FID) [5], CLIP Score (CLIP) [11], Human Preference Score (HPS) [16] and LPIPS distance (LPIPS) [21].

FID measures the feature distributions similarity between generated and real images. Lower FID values indicate better distribution matching (↓). **CLIP** quantifies the image-text alignment degree within the CLIP embedding space. A higher CLIP score reflects greater semantic alignment between the generated image and text prompt (↑). **HPS** measures the subjective quality of the generated images based on human evaluations. Higher HPS values suggest that the generated images are more favorable or preferred by human evaluators (↑). **LPIPS** quantifies the appearance deviation between the generated image and the input condition. A higher LPIPS means the generated image with richer appearance details (↑).

4.1.3. Implementation details

In the implementation of our proposed Subjective Camera, we set the learning rate η in Eq. 3 and the threshold parameter τ in Eq. 4 is 5.0 and 0.3, respectively. Meanwhile, hyper-parameters α_i , β_i and γ in Eq. 5 is set as 0.8, 0.2 and 0.9, respectively. The factor that controls intensity μ in Eq. 11 is set as 5.0. Our method is preformed on one NVIDIA GeForce RTX 4090 and input sketch images are 512×512 in resolution.

4.2. Comparison With Baselines

We conducted a comprehensive quantitative and qualitative evaluation of the proposed method and comparison methods on the CMC and FMC datasets, with the quantitative results presented in Table 1. And qualitative results on our FMC and CMC dataset are shown in Figure 1 and Figure 3.

We observe that training-based methods (e.g., ControlNet [20], T2I-Adapter [10], and Uni-ControlNet [24]), are susceptible to subjective bias in sketches and fail to adhere strictly to text prompts, resulting in unrealistic images and lower CLIP scores. Training-free methods [1, 4, 9] suffer from concepts omissions, presence of conspicuous artifacts & background absence, and inconsistencies between concepts & background, leading to unrealistic image generation. This is attributed to the fact that these training-free methods neglect to bridge the modality gap and are further compromised by mutual interference during multi-concept generation, resulting in unrealistic images, inferior image-text alignment, and more significant appearance deviations. On the contrary, our proposed Subjective Camera faithfully reconstruct real-world physical scenes and achieves the best performance across all evaluation metrics on both the CMC & FMC datasets, demonstrating its effectiveness.

4.3. Ablation Study

To validate the effectiveness of each module in our method, we conducted ablation experiments on the FMC and CMC datasets, with the visualization results shown in Figure 4.

It is observed that traditional T2I diffusion models (T2I) generate images that are close to text prompts. While incorporating sketches as guidance further constrains the consistency of concepts positioning, deviations in appearance and spatial alignment still persist (T2I, OP). The sequential concept understanding facilitated by Sequence-Aware Disentangled Generation (SADG) in Sec. 3.3 enhances the alignment of concept positioning and appearance with input sketches (T2I, SADG). Simultaneously, the Latent Optimization (OP) module in Sec. 3.4 aligns content latent variables with real-world objects, mitigating geometric misalignment (T2I, OP, LO). When integrating all modules, our method faithfully reconstructs real-world scenes and achieves optimal results (Ours), demonstrating the effectiveness of each module and underscoring the indispensable nature of their design.

4.4. User Preference Experiments

We invited 30 participants, including professional illustrators and individuals with little experience. Each participant was asked to depict a deeply impressive scene through both verbal description and sketching within two minutes. This process was repeated across three rounds, with participants illustrating the same scene each time. We then generated images using the optimal baseline [9], an ablated module of

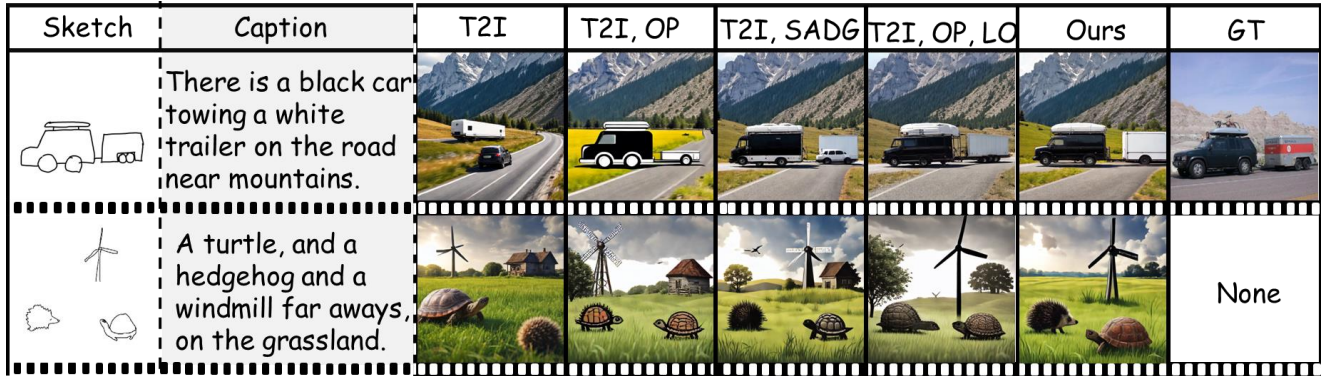


Figure 4. **Ablation study on CMC and FMC datasets.** Column headers are defined as follows: T2I denotes the baseline text-to-image diffusion model; OP (Overall Perception) indicates the single-step guidance approach utilizing complete sketch as a holistic conditioning signal; SADG refers to our proposed Sequence-Aware Disentangled Generation (Sec. 3.3); LO represents the Latent Optimization module (Sec. 3.4) that enhances structural plausibility by injecting diffusion priors into imperfect sketches. Qualitative comparison demonstrates that SADG achieves finer layout control than OP. While LO effectively bridges the domain gap between freehand sketches and physical reality through latent space regularization, ultimately elevating generation quality.

Baseline	11%	23%	66%
w/o Test-Reward	16%	42%	42%
w/o SADG	16%	11%	73%
Random Order	18%	38%	44%
w/o LO	23%	12%	65%

Figure 5. **The overall results of the user preference experiments.** Our model significantly outperforms the state-of-the-art baseline methods [9]. Furthermore, the results indicate that every design in our approach is necessary, with SADG playing a particularly crucial role. We also conducted a permutation experiment in this section by shuffling the order of user drawings before inputting them into SADG. The results demonstrate that users subjectively prefer the sequential use of SADG. The entire experiment was conducted in a single-blind manner for the users.

our method, and our full model. Participants were presented with paired comparisons and asked to select the image that better matched their impression of the scene (or indistinguishable).

We found that participants refined their language and sketching strategies across rounds, with semantic richness increasing, while the sequence of concepts in the drawing process remains. As shown in Figure 6 Overall, our approach significantly outperformed the comparative conditions in all cases, with the model’s capabilities becoming even more pronounced as the rounds progressed. Notably, in the third round, our full model exhibited a substantial improvement in textual description comparisons. These results demonstrate that our model excels not only under vague user input but also in accurately capturing more precise user intentions.

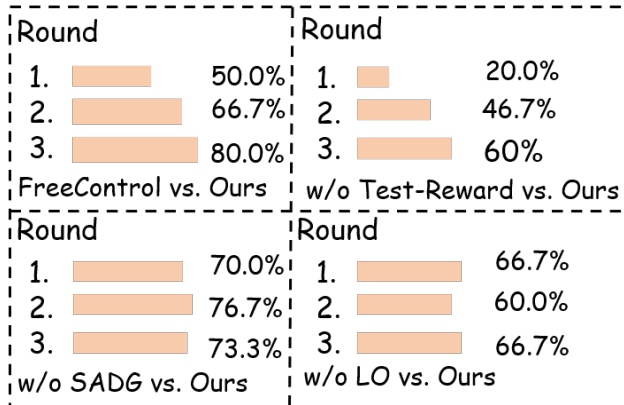


Figure 6. **The win rate of our model in each round of the user preference experiment.** Our win rate increases as users adjust their input strategies, allowing our model’s capabilities to be further unleashed and improving the win rate compared to the baseline. The ablation study on the text reward module also shows a significant difference, demonstrating the importance of appearance priors provided by the richness of textual semantics. However, there is no noticeable difference between SADG and LO, as users rarely adjust their drawing order, and the drawing results remain relatively stable within the limited time.

5. Conclusions

In this paper, we introduce Subjective Camera, a novel paradigm that enables users to reconstruct real-world scenes based on mental impressions, leveraging synergy between progressive freehand sketches and textual descriptions. Unlike existing methods that either require costly fine-tuning of text-to-image diffusion models or struggle with sketch quality dependence and geometric misalignment, our

framework effectively addresses these challenges through a training-free, sequence-aware generative process.

Through extensive experiments on both synthetic (CMC dataset) and real-world (FMC dataset) human-drawn sketches, we demonstrate that Subjective Camera achieves state-of-the-art performance, outperforming both training-free and training-based sketch-to-image generation methods in terms of FID, CLIP score, user preference (HPS), and structural consistency (LPIPS).

References

- [1] Zhenwei Cheng, Lei Wu, Changshuo Wang, and Xiangxu Meng. Scene sketch-to-image synthesis based on multi-object control. In *ICASSP 2024-2024 IEEE International Conference on Acoustics, Speech and Signal Processing (ICASSP)*, pages 3775–3779. IEEE, 2024. 1, 2, 3, 6, 7
- [2] Luca Eyring, Shyamgopal Karthik, Karsten Roth, Alexey Dosovitskiy, and Zeynep Akata. Reno: Enhancing one-step text-to-image models through reward-based noise optimization. *Advances in Neural Information Processing Systems*, 37:125487–125519, 2025. 3
- [3] Xiefan Guo, Jinlin Liu, Miaomiao Cui, Jiankai Li, Hongyu Yang, and Di Huang. Initno: Boosting text-to-image diffusion models via initial noise optimization. In *Proceedings of the IEEE/CVF Conference on Computer Vision and Pattern Recognition*, pages 9380–9389, 2024. 3
- [4] Amir Hertz, Ron Mokady, Jay Tenenbaum, Kfir Aberman, Yael Pritch, and Daniel Cohen-or. Prompt-to-prompt image editing with cross-attention control. In *The Eleventh International Conference on Learning Representations*. 6, 7
- [5] Martin Heusel, Hubert Ramsauer, Thomas Unterthiner, Bernhard Nessler, and Sepp Hochreiter. Gans trained by a two time-scale update rule converge to a local nash equilibrium. *Advances in neural information processing systems*, 30, 2017. 7
- [6] Yuval Kirstain, Adam Polyak, Uriel Singer, Shahbuland Matiana, Joe Penna, and Omer Levy. Pick-a-pic: An open dataset of user preferences for text-to-image generation. *Advances in Neural Information Processing Systems*, 36: 36652–36663, 2023. 3
- [7] Seung Hyun Lee, Yinxiao Li, Junjie Ke, Innfarn Yoo, Han Zhang, Jiahui Yu, Qifei Wang, Fei Deng, Glenn Entis, Junfeng He, et al. Parrot: Pareto-optimal multi-reward reinforcement learning framework for text-to-image generation. In *European Conference on Computer Vision*, pages 462–478. Springer, 2024. 3
- [8] Xingyue Lin, Xingjian Hu, Shuai Peng, Jianhua Zhu, and Liangcai Gao. Sketchref: A benchmark dataset and evaluation metrics for automated sketch synthesis. *arXiv preprint arXiv:2408.08623*, 2024. 2
- [9] Sicheng Mo, Fangzhou Mu, Kuan Heng Lin, Yanli Liu, Bochen Guan, Yin Li, and Bolei Zhou. Freecontrol: Training-free spatial control of any text-to-image diffusion model with any condition. In *Proceedings of the IEEE/CVF Conference on Computer Vision and Pattern Recognition*, pages 7465–7475, 2024. 1, 3, 6, 7, 8
- [10] Chong Mou, Xintao Wang, Liangbin Xie, Yanze Wu, Jian Zhang, Zhongang Qi, and Ying Shan. T2i-adapter: Learning adapters to dig out more controllable ability for text-to-image diffusion models. In *Proceedings of the AAAI Conference on Artificial Intelligence*, pages 4296–4304, 2024. 1, 2, 3, 6, 7
- [11] Alec Radford, Jong Wook Kim, Chris Hallacy, Aditya Ramesh, Gabriel Goh, Sandhini Agarwal, Girish Sastry, Amanda Askell, Pamela Mishkin, Jack Clark, et al. Learning transferable visual models from natural language supervision. In *International conference on machine learning*, pages 8748–8763. PmLR, 2021. 7
- [12] Robin Rombach, Andreas Blattmann, Dominik Lorenz, Patrick Esser, and Björn Ommer. High-resolution image synthesis with latent diffusion models. In *Proceedings of the IEEE/CVF conference on computer vision and pattern recognition*, pages 10684–10695, 2022. 3
- [13] Patsorn Sangkloy, Nathan Burnell, Cusuh Ham, and James Hays. The sketchy database: learning to retrieve badly drawn bunnies. *ACM Transactions on Graphics (TOG)*, 35(4):1–12, 2016. 6
- [14] Aravindan Sundaram, Ujjayan Pal, Abhimanyu Chauhan, Aishwarya Agarwal, and Srikrishna Karanam. Cocono: Attention contrast-and-complete for initial noise optimization in text-to-image synthesis. *arXiv preprint arXiv:2411.16783*, 2024. 3
- [15] Narek Tumanyan, Michal Geyer, Shai Bagon, and Tali Dekel. Plug-and-play diffusion features for text-driven image-to-image translation. In *Proceedings of the IEEE/CVF Conference on Computer Vision and Pattern Recognition*, pages 1921–1930, 2023. 1, 7
- [16] Xiaoshi Wu, Keqiang Sun, Feng Zhu, Rui Zhao, and Hongsheng Li. Human preference score: Better aligning text-to-image models with human preference. In *Proceedings of the IEEE/CVF International Conference on Computer Vision*, pages 2096–2105, 2023. 7
- [17] Zhenbei Wu, Haoge Deng, Qiang Wang, Di Kong, Jie Yang, and Yonggang Qi. Sketchscene: Scene sketch to image generation with diffusion models. In *2023 IEEE International Conference on Multimedia and Expo (ICME)*, pages 2087–2092. IEEE, 2023. 2, 3
- [18] Jiazheng Xu, Xiao Liu, Yuchen Wu, Yuxuan Tong, Qinkai Li, Ming Ding, Jie Tang, and Yuxiao Dong. Imagereward: Learning and evaluating human preferences for text-to-image generation. *Advances in Neural Information Processing Systems*, 36:15903–15935, 2023. 3
- [19] Qian Yu, Jifei Song, Yi-Zhe Song, Tao Xiang, and Timothy M Hospedales. Fine-grained instance-level sketch-based image retrieval. *International Journal of Computer Vision*, 129(2):484–500, 2021. 2
- [20] Lvmin Zhang, Anyi Rao, and Maneesh Agrawala. Adding conditional control to text-to-image diffusion models. In *Proceedings of the IEEE/CVF International Conference on Computer Vision*, pages 3836–3847, 2023. 1, 2, 3, 6, 7
- [21] Richard Zhang, Phillip Isola, Alexei A Efros, Eli Shechtman, and Oliver Wang. The unreasonable effectiveness of deep features as a perceptual metric. In *Proceedings of the IEEE conference on computer vision and pattern recognition*, pages 586–595, 2018. 7
- [22] Tianyu Zhang and Haoran Xie. Sketch-guided text-to-image generation with spatial control. In *2024 2nd International Conference on Computer Graphics and Image Processing (CGIP)*, pages 153–159. IEEE, 2024. 2, 3
- [23] Tianyu Zhang, Xiaoxuan Xie, Xusheng Du, and Haoran Xie. Sketch-guided scene image generation. *arXiv preprint arXiv:2407.06469*, 2024. 2, 3
- [24] Shihao Zhao, Dongdong Chen, Yen-Chun Chen, Jianmin Bao, Shaozhe Hao, Lu Yuan, and Kwan-Yee K Wong. Uni-controlnet: All-in-one control to text-to-image diffusion

models. *Advances in Neural Information Processing Systems*, 36:11127–11150, 2023. [1](#), [2](#), [3](#), [6](#), [7](#)